Microsyst Technol (2013) 19:1919–1925
DOI 10.1007/s00542-013-1763-6

TECHNICAL PAPER

# Gas-mass-flow transfer-rate simulation and experimental evaluation in microchannels

**G. P. Patsis · K. Ninos · D. Mathioulakis · G. Kaltsas**

Received: 28 August 2012 / Accepted: 2 March 2013 / Published online: 21 March 2013


**Abstract** Continuum hydrodynamics accurately describes the flow of fluids over a wide range of systems. However, continuum models are unable to adequately describe the flow of fluid under extreme confinement. In particular, the no-slip boundary condition invoked in continuum flow calculations is violated for low density gases flowing in microtubes or nanoporous materials. The calculation of gas-mass-transfer rate in microtubes using experiments and simulation is investigated in the case of small absolute pressures. Specifically, in the present work, Argon, Helium, and Air gas is considered in a 3D model of two metallic tanks connected through microchannels. The pressure difference between the inlet and the outlet of the structure is monitored as a function of time. Thus the gas- transfer-rate is evaluated and compared with experimental data, in order to verify the departure from the standard Navier–Stokes equations with the no-slip boundary condition.

**List of symbols**

| | |
|---|---|
| $\rho$ | Fluid's density (kg/m$^3$) |
| $\vec{u}$ | Velocity vector (m/s) |
| $p$ | Pressure (Pa) |
| $F$ | Volume force (kg m s$^{-2}$) |
| $M$ | Molecular weight of gas |
| $\mu$ | Dynamic viscosity (Pa s) |
| $\lambda$ | Mean free path (m) |
| $\vec{I}$ | Unity matrix |
| $R$ | Gas constant (J/kg K) |
| $T$ | Absolute temperature (K) |
| $m$ | Gas mass in the metallic tank (kg) |
| $V$ | Metallic tank volume (m$^3$) |
| $\Delta u\|_w$ | Tangential velocity slip at the wall |
| $L_s$ | Constant slip length |
| $\frac{\partial u}{\partial y}\|_w$ | Strain rate computed at the wall |
| $a_v$ | Tangential momentum-accommodation coeffi cient |
| $\tau_{n,t}$ | Shear stress along the boundary (Pa) |
| $R_n = \frac{\rho u L}{\mu}$ | Reynolds number |
| $K_n = \frac{\lambda}{L}$ | Knudsen number |

G. P. Patsis (✉) · K. Ninos · G. Kaltsas
Department of Electronics, TEI of Athens, Athens, Greece
e-mail: patsisg@teiath.gr

D. Mathioulakis
School of Mechanical Engineering, NTUA, Athens, Greece

## 1 Introduction

Calculation of mass flow rate of gases in micro channels under small absolute pressures deviates from experimental findings when the theory of continuum mechanics is applied. This deviation becomes evident when Knudsen number takes values above 0.1, namely when the gas is considered as rarefied (Shen 2005). Under these conditions, the number of atom collisions with the internal wall of the tube has to be taken into consideration. In fact, the failure of the continuum model happens when the shear stress and the heat flux in the continuum equations of mass, momentum and energy conservation can no longer be characterized by the macroscopic magnitudes of lower order (velocity, temperature) i.e., when the expressions of the transport coefficients are no longer valid. This occurs when the scale length of the gradients of the macroscopic quantities becomes so small that it is comparable with the molecular mean free path of the gas (Shen 2005). The scale length of the gradients of the macroscopic magnitudes is:

**Table 1** Different Knudsen number regimes

| Equation System | Knudsen Number | Fluid Model |
|---|---|---|
| Euler equations | $K_n \to 0$, $R_n \to \infty$ | Continuum, neglect molecular diffusion |
| Navier–Stokes equations with no–slip boundary conditions | $K_n < 10^{-3}$ | Continuum with molecular diffusion |
| Navier–Stokes equations with slip boundary conditions | $10^{-3} \leq K_n < 10^{-1}$ | Continuum, transition |
| Moment equations, direct simulation Monte Carlo (DSMC), Lattice Boltzmann | $10^{-1} \leq K_n < 10$ | Transition regime |
| DSMC, Lattice Boltzmann | $K_n \geq 10$ | Free-molecule flow |

$$L = \rho/(d\rho/dx) \quad (1)$$

To characterize the degree of rarefaction the Knudsen number is introduced and is defined as the ratio of the molecular mean free path $\lambda$ (the average distance traveled by a molecule between two collisions) and the characteristic length of the flow $L$:

$$K_n = \lambda/L \quad (2)$$

Tsien (1946) divides the rarefied gas flows into three realms according to the degree of rarefaction, i.e., the slip flow regime, the transitional regime and the free molecular regime. The different Knudsen number regimes are summarized in Table 1 (Gad-el-Hak 2002).

For macroscopic devices, the Knudsen number is very small, so the surrounding gas can be treated as a continuous medium. However, in microscale, the Knudsen number can be fairly large due to the small $L$. In micron and submicron scales, momentum and energy transport show significant deviations from their larger scale counterparts.

Rarefied gas flows are encountered in small geometries such as micro-electro-mechanical-devices (MEMS). MEMS operate in a wide variety of flow regimes covering the continuum, slip and early transitional flow regimes. Further miniaturization of MEMS device components and nanotechnology applications correspond to higher Knudsen numbers, making it necessary to study the mass, momentum and energy transport in the entire Knudsen regime. Figure 1 shows some MEMS examples and the various regimes of Knudsen number for comparison.

Although a molecular-simulation-based approach for understanding fluid forces on surfaces is fundamental in nature, it is very difficult to apply such simulation to engineering problems due to the vast number of molecules involved in the analysis; however, direct application of the well-known continuum equations is not appropriate, either. The aim of the current work is therefore threefold:

1. Test the simulation limitations of the Navier–Stokes equations in the transition region of Knudsen numbers for rarefied gas flows.
2. Create a practical model for measuring mass flow in microchannels that will enable improvements in subsequent physical modeling for accurate predictions.

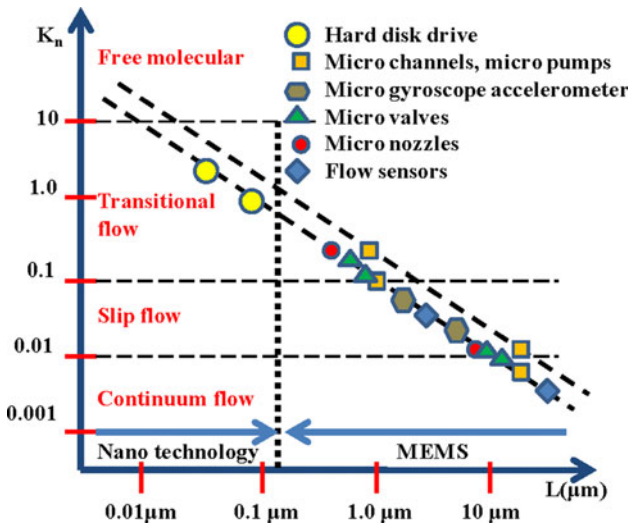


**Fig. 1** The Operation range for typical MEMS and nanotechnology applications under standard conditions spans the entire Knudsen regime (continuum, slip, transition and free molecular flow regimes)

3. Test the current level of model development against corresponding experimental data for comparison.

In Sect. 2, the apparatus for the experimental determination of mass-flow-rate of rarefied gases is described. Following in Sect. 3, the way towards a 3D model development for the measurement of gas mass-transfer-rate in microchannels is presented. Finally, comparison with the experimental mass flow rate measurements is performed along with the corresponding discussion.

## 2 Experimental procedure and materials

The flow of three gases, namely Argon, Helium and Air through microchannels was examined. Six devices were fabricated by Chipshop, GmbH (http://www.microfluidic-chipshop.com/), each including eight parallel 5,000 μm long channels, connecting two tanks with dimensions 12 mm width by 6 mm length and 100 μm height each. The structure material was PMMA. The micro channels height was 20 μm for the first three devices and 30 μm for the other three devices. The average width of the channels

was 285 μm. According to one point measurements, it was found that in each device the maximum variation in the depth and width of the channels was in the worst case 4 and 12 μm, respectively. Each tank of the micro device was connected to a 35 ml steel tank via a 300 mm long tube with 1.6 mm diameter. Figure 2a shows the overall geometry of the experimental apparatus and Fig. 2b a magnified view of one microchannel's output.

One of the latter tanks was filled with gas at a predefined pressure, which was determined by an absolute capacitive pressure transducer (CERAVAC, CTR 90, Leybold Vakuum GmbH, range 0.01–100 Torr). The other metallic tank was connected to a vacuum pump (GEV, 3/GP1, minimum pressure = 0.5 mbar), keeping the pressure at the exit of the channels at 1 Torr. The pressure at the micro device outlet was measured with another absolute capacitive pressure transducer (Baratron 722A, max. pressure = 20 Torr). The overall duration of the specific experiment was less than an hour, thus it is assumed that the reference temperature was varying no more than 0.5 °C around 25 °C which was the room temperature.

The experimental procedure was as follows: after filling one of the metallic tanks with gas supplied from a container at a pressure of about 90 Torr, the other tank was connected to the vacuum pump, thus establishing gas flow through the micro channels. Practically the same pressure difference as that of the metallic tanks was applied at the inlet and outlet of the channels since the pressure drop between the metallic tanks and the micro device was estimated to be a fraction of a Torr by the application of the Darcy-Weisbach formula. The pressure signals were recorded with a frequency of 10 Hz using a 16 bit A/D converter. The pressure of the tank with the higher pressure was recorded with a resolution of 1.5 mTorr (100 Torr/216) which coincided with the resolution of the transducer.

The mass flow rate was calculated using the pressure of the higher pressure metallic tank and the perfect gas law, considering that the pressure reduction rate equals the mass-flow-rate entering the micro device. Thus:

$$\frac{dm}{dt} = \frac{dp}{dt}\frac{V}{RT} \tag{3}$$

The pressure time-derivative was based on a curve fitted on the pressure function.

## 2.1 Model development

Initially a 2D model of the channel profile was simulated, namely along its length x = 5000 μm and its depth z = 300 μm. Inlet and outlet pressure is 13332 Pa and 133.32 Pa, respectively.

The simulation was performed in COMSOL (www.comsol.com) using the finite element technique. The weakly compressible Navier–Stokes equations (WCNSE) are used and they are given by:

$$\rho\left(\vec{u}\cdot\vec{\nabla}\right)\vec{u} = \vec{\nabla}\left[-p\,\underset{\sim}{I} + \mu\left(\vec{\nabla}\vec{u} + \left(\vec{\nabla}\vec{u}\right)^{T}\right) - \frac{2}{3}\mu\left(\vec{\nabla}\vec{u}\right)^{T}\underset{\sim}{I}\right] + \vec{F} \tag{4}$$

and

$$\vec{\nabla}(\rho\vec{u}) = 0 \tag{5}$$

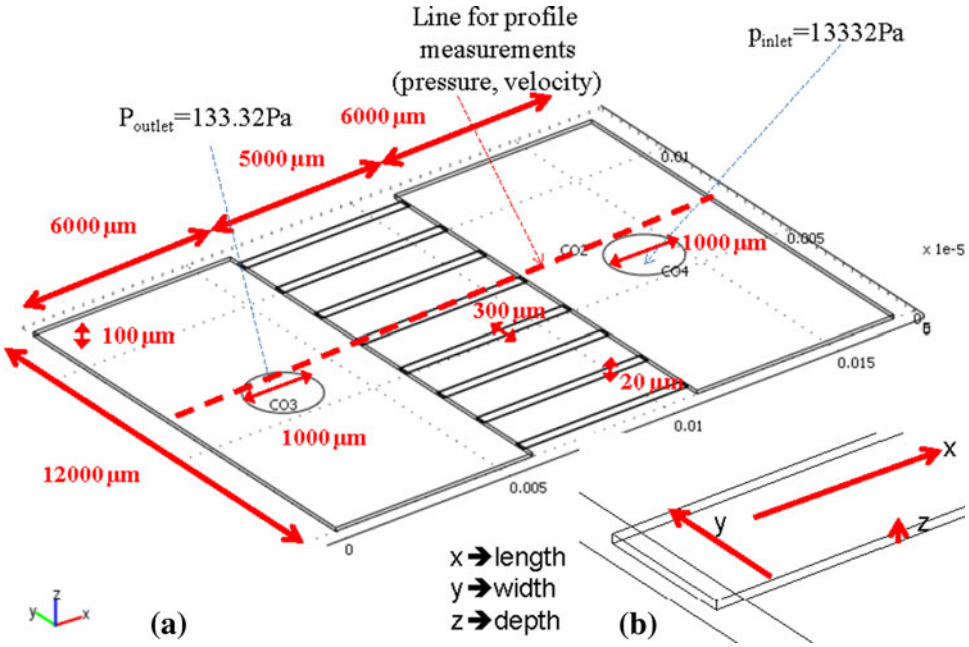


**Fig. 2** **a** Simulation geometry. **b** Magnified view of one microchannel outlet

In microscale, there is a slip velocity at the boundary. For both liquids and gases, the linear Navier boundary condition empirically relates the tangential velocity-slip at the wall $\Delta u|_w$ to the local shear:

$$\Delta u|_w = u_{fluid} - u_{wall} = L_s \frac{\partial u}{\partial y}|_w \quad (6)$$

In most practical situations, the slip length is so small that the no-slip condition holds. In MEMS applications however, that may not be the case.

Assuming isothermal conditions prevail, the above slip relation has been rigorously derived by Maxwell in 1879 from considerations of the kinetic theory of dilute, monatomic gases. Gas molecules, modeled as rigid spheres, continuously strike and reflect from a solid surface, just as they continuously collide with each other. For an idealized perfectly smooth wall (at the molecular scale), the incident angle exactly equals the reflected angle and the molecules conserve their tangential momentum and thus exert no shear on the wall. This is termed specular-reflection which results in perfect slip at the wall. For an extremely rough wall, on the other hand, the molecules reflect at some random angle uncorrelated with their entry angle. This perfectly diffuse reflection results in zero tangential momentum for the reflected fluid molecules to be balanced by a finite slip velocity in order to account for the shear stress transmitted to the wall. A force balance near the wall leads to the following expression for the slip velocity:

$$u_{gas} - u_{wall} = \lambda \frac{\partial u}{\partial y}|_w \quad (7)$$

The right-hand side can be considered as the first term in an infinite Taylor series, sufficient if the mean free path is relatively small enough. The equation above states that significant slip occurs only if the mean velocity of the molecules varies appreciably over a distance of one mean free path. This is the case, for example, in vacuum applications and/or flow in microdevices. The number of collisions between the fluid molecules and the solid in those cases is not large enough for even an approximate equilibrium to be established. Furthermore, additional (nonlinear) terms in the Taylor series would be needed as $\lambda$ increases and the flow is further removed from the equilibrium state.

For real walls some molecules reflect diffusively and some reflect secularly. In other words, a portion of the momentum of the incident molecules is lost to the wall and a (typically smaller) portion is retained by the reflected molecules. The tangential-momentum-accommodation coefficient $a_v$ is defined as the fraction of molecules reflected diffusively. This coefficient depends on the fluid, the solid and the surface finish and has been determined experimentally to be between 0.2 and 0.9, the lower limit being for exceptionally smooth surfaces while the upper limit is typical of most practical surfaces. The final

**Table 2** Parameters for 2D simulation with Ar gas for use in COMSOL

| Parameter name | Parameter symbol | Parameter value |
|---|---|---|
| Channel length | $x$ | 5,000 μm |
| Channel depth | $z$ | 300 μm |
| Inlet pressure | pin | 13,332 Pa |
| Outlet pressure | Pout | 133.32 Pa |
| Dynamic viscosity Ar | muAr | 2.28E−5 [kg/m/s] |
| Average pressure | p2 | (pin + pout)/2 |
| | psqr2 | (p2 + 1)*(p2 + 1) |
| Density of Ar | rhoAr2 | (p2 + 1) [kg/m^3/Pa]* 0.039948/8.314/293 |
| Mean free path for Ar | lamAr | muAr*sqrt (3.14/ (2*rhoAr*(p2 + 1))) |

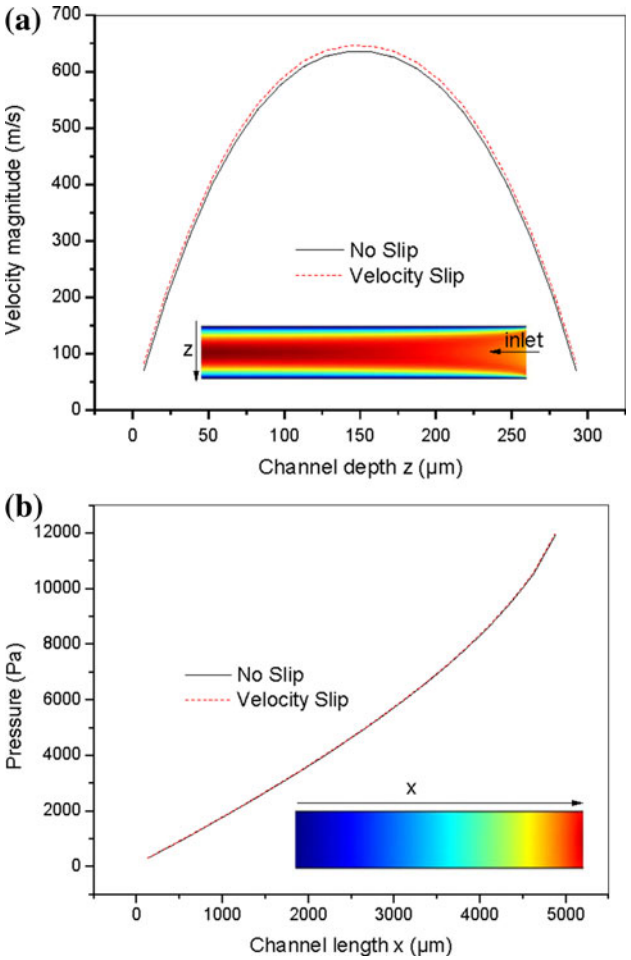


**Fig. 3** **a** Velocity profiles along channel depth. **b** Pressure profile along channel length x (*inlet is on the right and outlet on the left*). Gas is Argon. Results are from stationary analysis for a 2D model of a microchannel with and without slip boundary conditions (x = 5000 μm, z = 20 μm)

expression derived by Maxwell for an isothermal wall reads:

$$u_{gas} - u_{wall} = \frac{2 - a_v}{a_v} \lambda \frac{\partial u}{\partial y}|_w \tag{8}$$

For $a_v = 0$, the slip velocity is unbounded, while for $a_v = 1$:

$$u_{gas} - u_{wall} = \lambda \frac{\partial u}{\partial y}|_w \tag{9}$$

The following equation relates the viscosity-induced jump in tangential velocity to the tangential shear stress along the boundary, and is also implemented in COMSOL:

$$\Delta u = \frac{1}{\beta} \tau_{n.t} \tag{10}$$

For gaseous fluids, the coefficient $\beta$ equals:

$$\beta = \frac{\mu}{\left(\frac{2-a_v}{a_v}\right)\lambda} = \frac{\mu}{L_s} \tag{11}$$

With:

$$L_s = \left(\frac{2 - a_v}{a_v}\right)\lambda \tag{12}$$

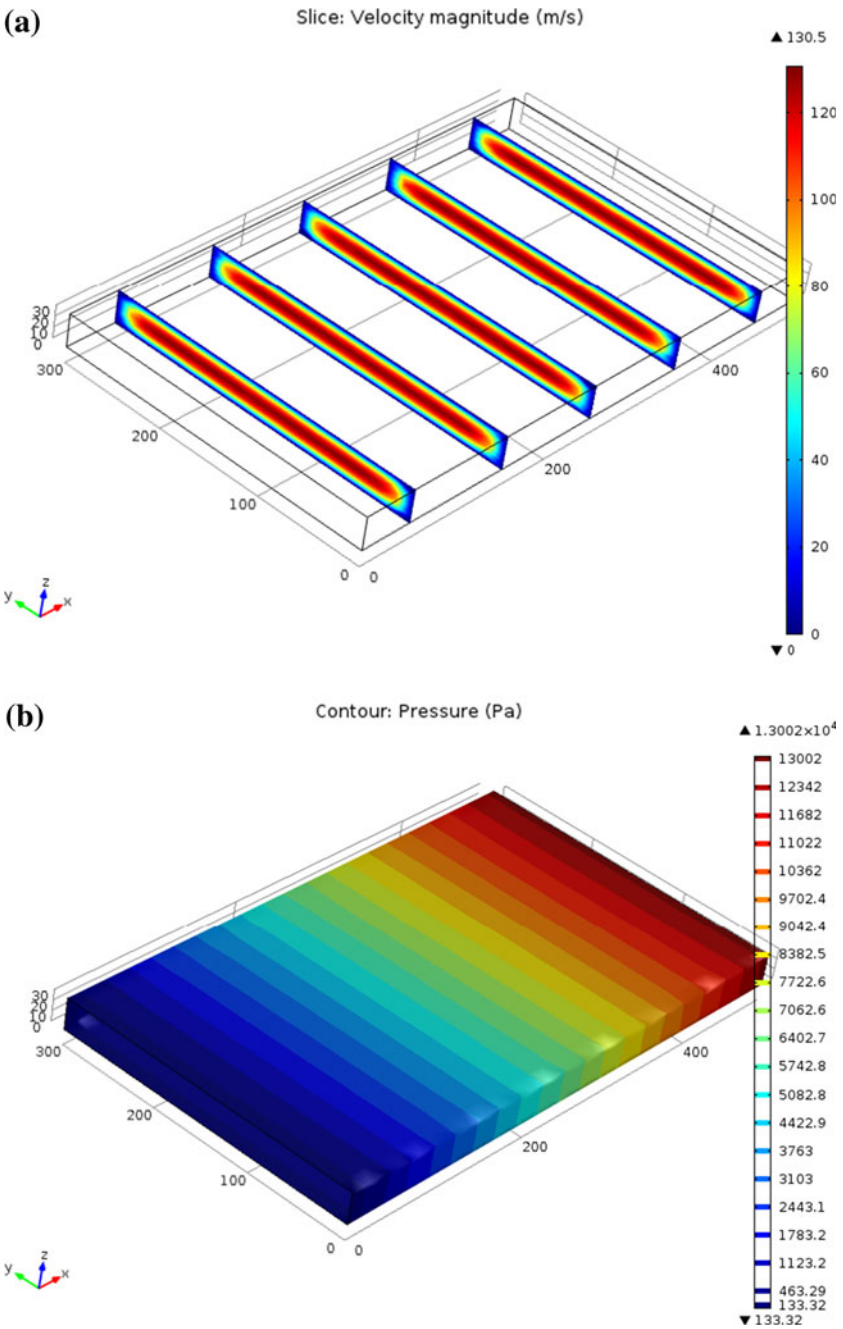


**Fig. 4** **a** Velocity value distribution. **b** Pressure distribution. Microchannel dimensions are 5000 μm by 300 μm by 30 μm. Gas is Argon. The same set of Eqs. (4) and (5) is used under no-slip boundary conditions

$$\lambda = \mu\sqrt{\frac{\pi}{\rho p}} \tag{13}$$

$L_s$ (the slip length) for a straight channel is a measure of the distance the flow profile extrapolates to zero away from the boundary. Equation (11) holds for both liquids and gases.

Both the no-slip and slip boundary conditions were used and the stationary situation is assumed (i.e. time derivatives set to zero). Room temperature conditions are considered i.e., $T = 293$ K. Density is a function of pressure through relation:

$$\rho = \frac{pM}{RT} \tag{14}$$

A 2D test of the WCNSE in COMSOL is considered next for a single microchannel with the simulation parameters of Table 2 for Argon. Figure 3 shows a comparison of the velocity magnitude along channel depth (Fig. 3a) and pressure along channel length (Fig. 3b).

Next a 3D model of one microchannel 5,000 μm by 300 μm by 30 μm was developed and tested under stationary conditions with the same set of WCNSE equations, under the no-slip boundary condition. Figure 4a shows slice plot of the velocity value distribution in the channel, while Fig. 4b illustrates the corresponding pressure field.

Finally, a complete 3D model of the experimental apparatus was developed as was seen in Fig. 2a which shows a 3D view of a structure with the two tanks and their connection to the microchannels, along with some geometric details. Figure 2b shows a magnified view of the microchannel/tank junction and the directions along which velocity and pressure profiles are recorded. In the next section the simulation results are presented and discussed based on the total 3D model of the experimental apparatus.

## 3 Results and discussion based on 3D model of the apparatus

Figure 5 shows an example of the velocity distribution near the outlet of the microchannel for the no-slip (Fig. 5a) and with velocity slip boundary condition (Fig. 5b) for Argon. Both plots indicate an increase in the fluid's velocity near the channel outlet.

Quantitative examples of velocity and pressure profile for He, Ar and Air as the flowing medium along $x$ and $z$ directions are shown in Figs. 6, 7, respectively. The mean free path and the slip length is a function of the position $x$, through the relations shown in the inset of Fig. 6.

Figure 8 with the continuous line shows the experimentally determined mass-flow-rate for Ar vs. the pressure difference between inlet and outlet. The simulation-results (discrete square points) in the case of Argon gas, are also

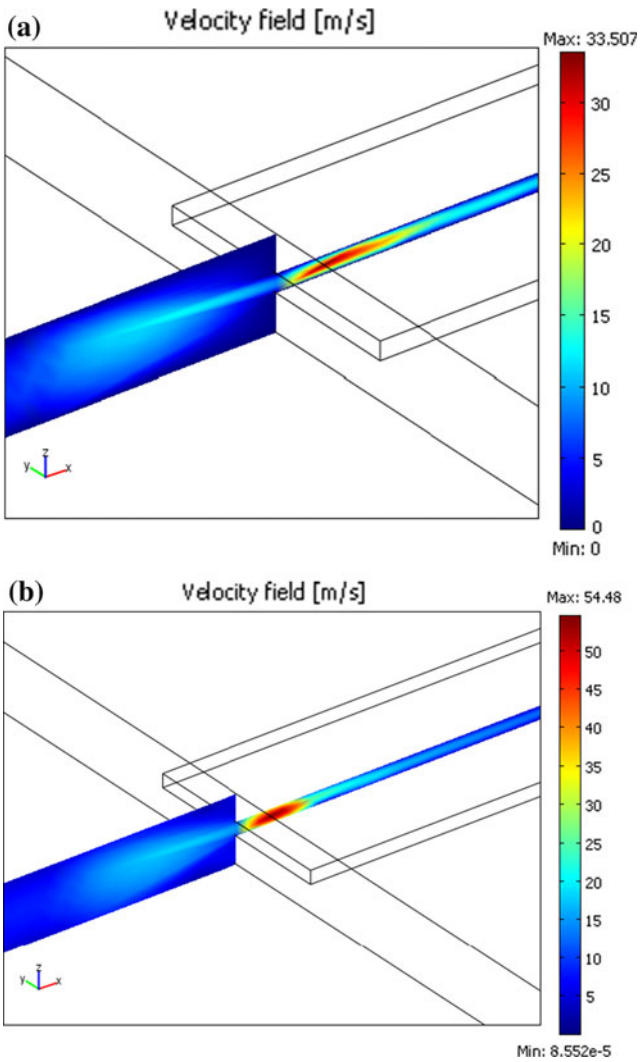


**Fig. 5** Velocity profile near outlet. **a** with no-slip. **b** With velocity slip. Gas is Ar. Stationary analysis results

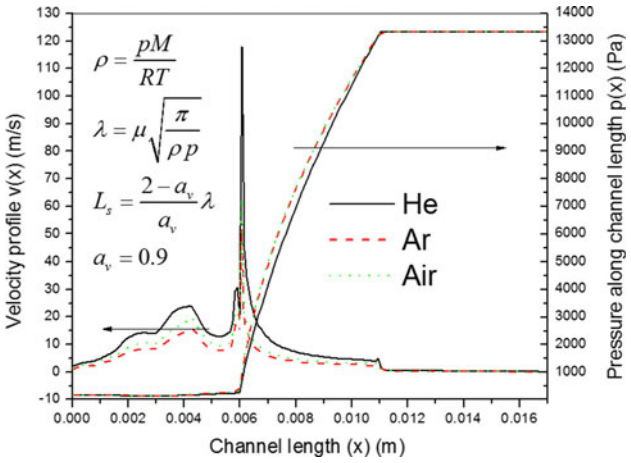


**Fig. 6** Velocity and pressure profile with velocity slip boundary condition along the center of one micro-channel, for He, Air and Ar as flowing medium. Outlet is at x = 0.0 and inlet at x = 0.015 m

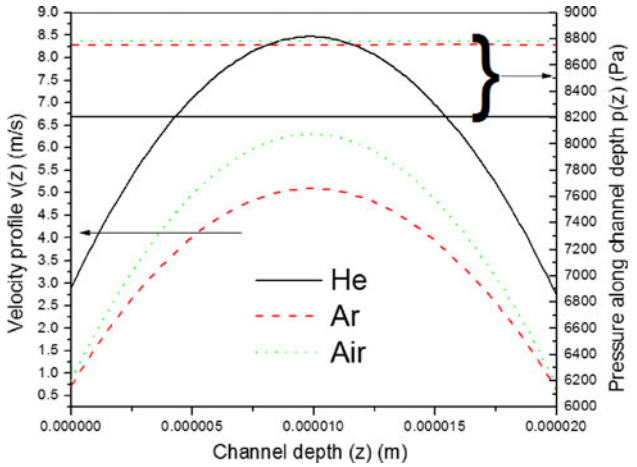


**Fig. 7** Velocity and pressure profile with velocity slip boundary condition along the channel depth of one micro-channel, for He, Air and Ar as flowing medium

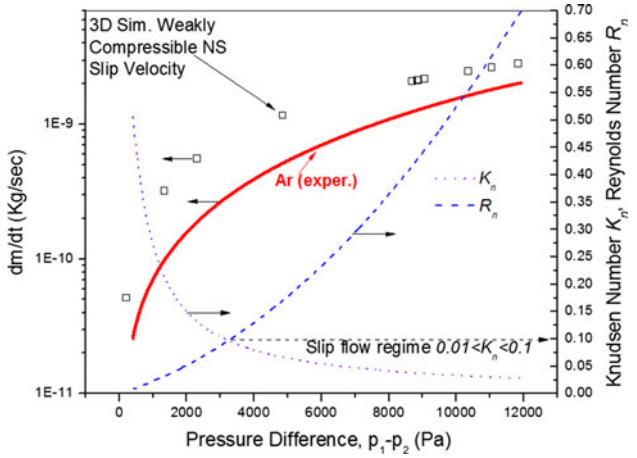


**Fig. 8** Comparison of experimental and simulated mass transfer rate. Knudsen and Reynolds numbers obtained using the experimental measurements of pressure differences in the two tanks

shown. (Velocity and pressure fields and their profiles in various sections of the simulated structure were used to obtain these data). The slip-flow regime in the pressure range is extracted from $K_n$ which is shown along with Reynolds number $R_n$ for reference, in the right axis of Fig. 8.

Reynolds number describes the importance of the "convective" inertia term in relation to viscosity in the Navier–Stokes equations themselves. In general, as the length scale $L$ of the fluid flow is reduced, properties that scale with the surface area of the system become comparatively more important than those that scale with the volume of the flow. This is apparent in the fluid flow itself as the viscous forces, which are generated by shear over the isovelocity surfaces (scaling as $L^2$), dominate over the inertial forces (which scale volumetrically as $L^3$). The Reynolds number $R_n$, which characterizes the ratio of these two forces, is typically low, so the flow is laminar. In many cases the creeping (Stokes) flow regime applies ($R_n \ll 1$). Laminar flow typically occurs at Reynolds numbers less than 1,000.

What is concluded from the presentation of data in Fig. 8 is that numerical predictions for the gas mass-flow-rate, although they agree in order of magnitude, and follow roughly the shape of the experimental curve, they seem to overestimate the effect of pressure difference compared to the experimental measurements.

Such deviation is attributed to the limitations of the WCNSE along with the velocity slip boundary condition and to the computational grid which most probably has to be denser. For a more accurate description computational results should be obtained by solving the Boltzmann equation and the BGK model of molecule collisions (Varoutis et al. 2009; Pitakarnnop et al. 2010) (The BGK (Bhatnagar, Gross and Krook) model proposed in 1954 became the most important model to solve the integro-differential Boltzmann equation (proposed by Boltzmann in 1872).

## 4 Conclusions

The gas mass transfer rate in microtubes using experiments and simulation is investigated in the case of small absolute pressures. Finite element analysis software was used for the design and simulation of the model. It was verified that for $0.02 < K_n < 0.5$ i.e., for the slip regime and the begging of transient regime, the weakly compressible form of the Navier–Stokes equations with the velocity slip boundary condition on the structure walls, although it follows roughly the shape of the experimental mass-flow-rate, overestimates the effect of pressure difference. One should use more elaborate calculation methods.

## References

Gad-el-Hak M (ed) (2002) The MEMS Handbook. CRC Press
Pitakarnnop J, Varoutis S, Valougeorgis D, Geoffroy S, Baldas L, Colin S (2010) A novel experimental setup for gas microflows. Microfluid Nanofluid 8:57
Shen C (2005) Rarefied gas dynamics. Fundamentals, simulations and micro flows. Heat and mass transfer series, Springer, Verlag
Tsien HS (1946) Super aerodynamics, mechanics of rarefied gases. J Aero Sci 13:653
Varoutis S, Naris S, Hauer V, Day C, Valougeorgis D (2009) Computational and experimental study of gas flows through long channels of various cross sections in the whole range of the Knudsen number. J Vac Sci Technol 27(1):89